

# $\text{Li}_{0.99}\text{Ti}_{0.01}\text{FePO}_4/\text{C}$ composite as cathode material for lithium ion battery

Guan Wang · Yan Cheng · Manming Yan · Zhiyu Jiang

Received: 26 January 2006 / Revised: 30 January 2006 / Accepted: 9 May 2006 / Published online: 14 June 2006  
© Springer-Verlag 2006

**Abstract** Three kinds of  $\text{LiFePO}_4$  materials, mixed with carbon (as  $\text{LiFePO}_4/\text{C}$ ), doped with Ti (as  $\text{Li}_{0.99}\text{Ti}_{0.01}\text{FePO}_4$ ), and treated both ways (as  $\text{Li}_{0.99}\text{Ti}_{0.01}\text{FePO}_4/\text{C}$  composite), were synthesized via ball milling by solid-state reaction method. The crystal structure and electrochemical behavior of the materials were investigated using X-ray diffraction, SEM, TEM, cyclic voltammetry, and charge/discharge cycle measurements. It was found that the electrochemical behavior of  $\text{LiFePO}_4$  could be increased by carbon coating and Ti-doping methods. Among the materials,  $\text{Li}_{0.99}\text{Ti}_{0.01}\text{FePO}_4/\text{C}$  composite presents the best electrochemical behavior, with an initial discharge capacity of 154.5 mAh/g at a discharge rate of 0.2 C, and long charge/discharge cycle life. After 120 cycles, its capacity remains at 92% of the initial capacity. The  $\text{Li}_{0.99}\text{Ti}_{0.01}\text{FePO}_4/\text{C}$  composite developed here can be used as the cathode material for lithium ion batteries.

**Keywords**  $\text{LiFePO}_4$  · Ti-doping · Carbon · Cathode material · Lithium ion battery

## Introduction

Currently,  $\text{LiCoO}_2$  is the most widely used cathode material in commercial Li-ion batteries. But  $\text{LiCoO}_2$  is expensive, somewhat toxic, and has limited specific capacity, so research for finding more suitable cathode materials is very important. Recently, a series of materials with olivine

structures have been used as cathode materials for lithium ion batteries;  $\text{LiFePO}_4$  [1],  $\text{LiMnPO}_4$  [2],  $\text{LiNiPO}_4$  [3], and  $\text{LiCoPO}_4$  [3, 4] were included.  $\text{LiFePO}_4$  is the most attractive cathode material among these materials, which was developed by Goodenough and coworkers in 1997. It has the advantages of low cost, an abundance of raw materials, environmental benignity, high cycle stability, and a high theoretical capacity (168 mAh/g). However,  $\text{LiFePO}_4$  still cannot be used extensively due to its low electric conductivity and low electrochemical diffusion kinetics. When the charge and discharge processes of  $\text{LiFePO}_4$  are carried out at high rates, the capacity decreases significantly. Several methods are reported to improve the electrochemical diffusion kinetics of  $\text{LiFePO}_4$ . Andersson and Thomas [5] found that the diffusing properties of  $\text{LiFePO}_4$  could be improved with the decrease of the particle size, which may be due to the decrease of lithium ion diffusion distance among the small particles. Yamada et al. [6] reported that the discharge capacity of  $\text{LiFePO}_4$  can reach 95% of the theoretical value at a current density of 0.12 mA/cm<sup>2</sup> by using small particle materials.

To improve the conductivity of  $\text{LiFePO}_4$ , two efficient methods are proposed. One is adding carbon [7]. Huang et al. [8] reported that  $\text{LiFePO}_4/\text{C}$  (15 wt.%), which was prepared by heating the precursor composed of gel carbon and other starting raw materials, demonstrated excellent electrochemical properties. The capacity achieved 120 mAh/g, even discharged at a high discharge rate. However, a high amount of carbon addition will decrease the gravimetric and volumetric energy density of the materials. On the other hand, element doping has been considered as another efficient way for the enhancement of electronic conductivity in  $\text{LiFePO}_4$ . Many elements, such as Al [9], Mg [10], Zr, Nb, Ti [11–13], and Cr [14], have been used to dope  $\text{LiFePO}_4$  as  $\text{Li}_x\text{M}_{1-x}\text{FePO}_4$ , and the mecha-

G. Wang · Y. Cheng · M. Yan · Z. Jiang (✉)  
Department of Chemistry, and Shanghai Key Laboratory of Molecular Catalysis and Innovative Materials, Fudan University, Shanghai 200433, People's Republic of China  
e-mail: zyjjiang@fudan.ac.cn

nism for this doping has been studied [15–17]. Mg, Zr, Ti, [18, 19], Co, and Ni [20] have also been used to dope  $\text{LiFePO}_4$  as  $\text{LiFe}_x\text{M}_{1-x}\text{PO}_4$ . But the electrochemical properties of  $\text{LiFePO}_4$  need to be further improved to meet the requirement of practical lithium ion batteries at present.

Solid-state reaction is considered as the industrial method for the preparation of electrode materials due to its easy operation, although many other methods have been reported, such as sol-gel method [21], etc. In this paper,  $\text{Li}_{0.99}\text{Ti}_{0.01}\text{FePO}_4/\text{C}$  composite was firstly prepared by combining Ti doping with carbon coating method through solid-state reaction. The material presents a high discharge capacity and good cycle performance. It can be used as the cathode material for lithium ion batteries.

## Experimental

$\text{LiFePO}_4/\text{C}$  was synthesized using  $\text{LiOH}\cdot\text{H}_2\text{O}$ ,  $\text{FeC}_2\text{O}_4\cdot 2\text{H}_2\text{O}$ , and  $\text{NH}_4\text{H}_2\text{PO}_4$  as the raw materials in the mole ratio based on the formula of  $\text{LiFePO}_4$ . The starting materials, with added 5 wt.% acetylene black powder and a small amount of acetone, were milled by ball-milling at a rotating speed of 450 rpm for 6 h. The influence of the agate milling container and balls can be neglected. Then, the material was decomposed at 350 °C for 5 h in a flowing  $\text{Ar}+5\% \text{H}_2$  atmosphere. The decomposed products as precursors were pressed into pellets and sintered at different temperatures in the same atmosphere for 15 h.

To improve the electrochemical properties, the samples doped with low amounts of Ti (as  $\text{Li}_{0.99}\text{Ti}_{0.01}\text{FePO}_4$ ) and treated with both carbon coating and Ti doping (as  $\text{Li}_{0.99}\text{Ti}_{0.01}\text{FePO}_4/\text{C}$  composite) were prepared in a procedure similar to the previous one. Nanosized  $\text{TiO}_2$  powder was used as the doping material. All reagents are of analytical reagent degree.

A Bruker D8 Advanced X-ray diffractometer with  $\text{Cu K}\alpha$  radiation was used to identify the crystalline phase of the materials at a scan rate of 4.5 °/min. The morphology of the samples was measured using a Philips XL30 electron microscope. The thermogravimetric analysis (TGA, using Perkin Elmer, TGA 7) and differential thermal analysis (DTA, using Perkin Elmer, DTA 7) were used to investigate the synthesis process of  $\text{LiFePO}_4$  samples during the heat treatment. The TGA–DTA measurements were carried out in  $\text{Ar}+5\% \text{H}_2$  atmosphere with a heating rate of 5 °C  $\text{min}^{-1}$  from room temperature to 900 °C. Elemental compositions of samples (Li, Fe, P, and Ti) were determined by inductively coupled plasma (ICP) method.

The cyclic voltammetry measurement was carried out using a CHI660 electrochemical workstation in a three-chamber cell. The working electrode (surface area of 0.5  $\text{cm}^2$ ) consisted of 80 wt.% active material, 15 wt.% carbon black,

and 5 wt.% polytetrafluoroethylene binder. For three kinds of samples, each working electrode contained 4 mg of  $\text{LiFePO}_4$ -based material regardless of whether it contained C, Ti, or both. Both counter and reference electrodes were lithium sheets. All potentials presented in this paper correspond to the lithium electrode. The electrolyte was 1 M  $\text{LiPF}_6$ , ethylene carbonate, and dimethyl carbonate in 1:1 volume ratio electrolyte (Ferro Com.). The charge-discharge curves and the cycle stability of the samples were evaluated in model CR2016 coin cells, which consisted of a  $\text{LiFePO}_4$ -based positive electrode with the aforementioned composition, metal lithium foil negative electrode, and a celgard 2300 separator. Each composite positive electrode contained 20 mg of  $\text{LiFePO}_4$ -based material. The cells were assembled in a dry glove box. The charge–discharge cycling test was carried out galvanostatically at a different rate. The cut-off voltages for charge and discharge processes were 4.5 and 2.0 V, respectively. Experiments were carried out at room temperature.

## Results and discussion

*Structure of samples* Figure 1 shows the TGA and DTA curves of the precursor for preparing  $\text{Li}_{0.99}\text{Ti}_{0.01}\text{FePO}_4/\text{C}$  composites. There are five obvious weight loss stages in the TGA curve. The TGA curve can be analyzed by comparing it with the TGA curves (not shown here) of  $\text{LiOH}\cdot\text{H}_2\text{O}$ ,  $\text{FeC}_2\text{O}_4\cdot 2\text{H}_2\text{O}$ , and  $\text{NH}_4\text{H}_2\text{PO}_4$ . The weight loss at 50 °C corresponds to the loss of the remaining acetone and adsorbed water in the precursor. The dehydration of  $\text{LiOH}\cdot\text{H}_2\text{O}$  and  $\text{FeC}_2\text{O}_4\cdot 2\text{H}_2\text{O}$  occupies the temperature regions of 50–100 °C and 134–160 °C, respectively. The main weight loss in the temperature ranges 185–257 °C and 260–390 °C corresponds to the decomposition of

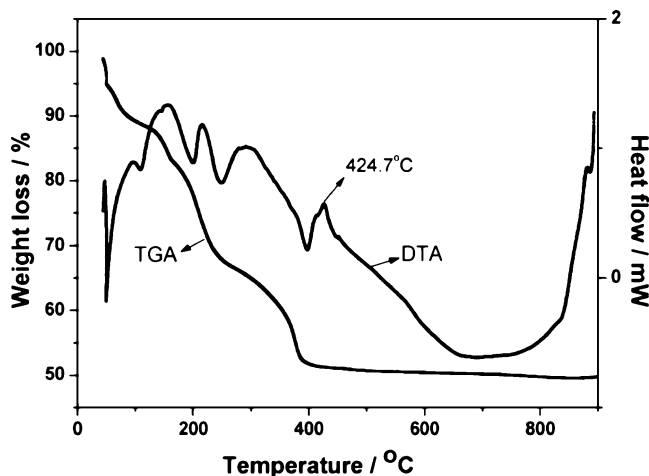


Fig. 1 TGA/DTA curves of the precursor for  $\text{Li}_{0.99}\text{Ti}_{0.01}\text{FePO}_4/\text{C}$  composite

$\text{NH}_4\text{H}_2\text{PO}_4$  and  $\text{FeC}_2\text{O}_4$ , respectively. Correspondingly, five endothermic peaks appear on the DTA curve below  $410^\circ\text{C}$ . When the temperature increases further, an exothermic peak appears at  $424.7^\circ\text{C}$ , which results in the formation of  $\text{LiFePO}_4$ . Therefore, the temperature for synthesizing  $\text{LiFePO}_4$  should be higher than  $425^\circ\text{C}$ . While further increasing the temperature, the TGA keeps almost a constant value until  $750^\circ\text{C}$ . Meanwhile, the DTA value decreases gradually to  $650^\circ\text{C}$ , and then becomes constant. It may reflect that the ordered olivine structure of  $\text{LiFePO}_4$  became more complete in this region. When the temperature is higher than  $750^\circ\text{C}$ , the DTA curve rises obviously. This rise may be caused by the production of some impurities at high temperature. The dopant  $\text{TiO}_2$  did not present obvious influence because the doping amount was very low.

The X-ray diffraction (XRD) patterns of  $\text{LiFePO}_4/\text{C}$  samples calcined at  $550$ ,  $650$ ,  $750$ , and  $850^\circ\text{C}$  are presented in Fig. 2a. The peaks of the sample synthesized at  $550^\circ\text{C}$  show the weakest intensity. All the peaks can be ascribed to ordered olivine crystalline  $\text{LiFePO}_4$  with an orthorhombic  $pnmb$  structure, except at  $2\theta=34^\circ$ , which corresponds to the impurity of  $\text{Fe}_3(\text{PO}_4)_2$ . This may indicate that the reaction is not completed at  $550^\circ\text{C}$ . Well-crystallized materials could be obtained at temperatures higher than  $650^\circ\text{C}$ . However, three peaks at  $2\theta=22.3$ ,  $23.2$ , and  $24.8^\circ$  (marked with stars) are observed at  $850^\circ\text{C}$ , which correspond to the impurity  $\text{Li}_3\text{PO}_4$ . This result is in agreement with the observation in thermal analysis experiments.

Figure 2b presents the XRD patterns for  $\text{LiFePO}_4/\text{C}$  (curve a) and  $\text{Li}_{0.99}\text{Ti}_{0.01}\text{FePO}_4/\text{C}$  (curve b) samples synthesized at  $750^\circ\text{C}$ . All XRD patterns present the character of ordered olivine-phase  $\text{LiFePO}_4$ . Table 1 lists the crystal parameters for these two samples. For the Ti-doped sample, parameter  $a$  decreases and  $c$  increases slightly, which may indicate the existence of Ti in the crystal lattice of  $\text{Li}_{0.99}\text{Ti}_{0.01}\text{FePO}_4$  [20].

The SEM images a, b, and c in Fig. 3 present the morphologies of  $\text{LiFePO}_4/\text{C}$ ,  $\text{Li}_{0.99}\text{Ti}_{0.01}\text{FePO}_4$ , and  $\text{Li}_{0.99}\text{Ti}_{0.01}\text{FePO}_4/\text{C}$  composite, respectively. It can be seen that, for the sample  $\text{LiFePO}_4/\text{C}$ , relative uniform submicron-size  $\text{LiFePO}_4$  particles were connected with carbon. Highly rotary ball-milling is helpful to prepare small-size particles. In addition, it has been known that the adding of carbon restrains the particle growth during lasting calcination [7, 22]. The particles of  $\text{Li}_{0.99}\text{Ti}_{0.01}\text{FePO}_4$  without carbon mixing are uneven with the particle size from several ten nanometers to more than  $200\text{ nm}$ . With carbon mixing, the particles of  $\text{Li}_{0.99}\text{Ti}_{0.01}\text{FePO}_4/\text{C}$  composite are uniform with a diameter of about  $100\text{ nm}$ , although they aggregated to form the grains in sizes of several hundred nanometers. A TEM image of  $\text{Li}_{0.99}\text{Ti}_{0.01}\text{FePO}_4/\text{C}$  compos-

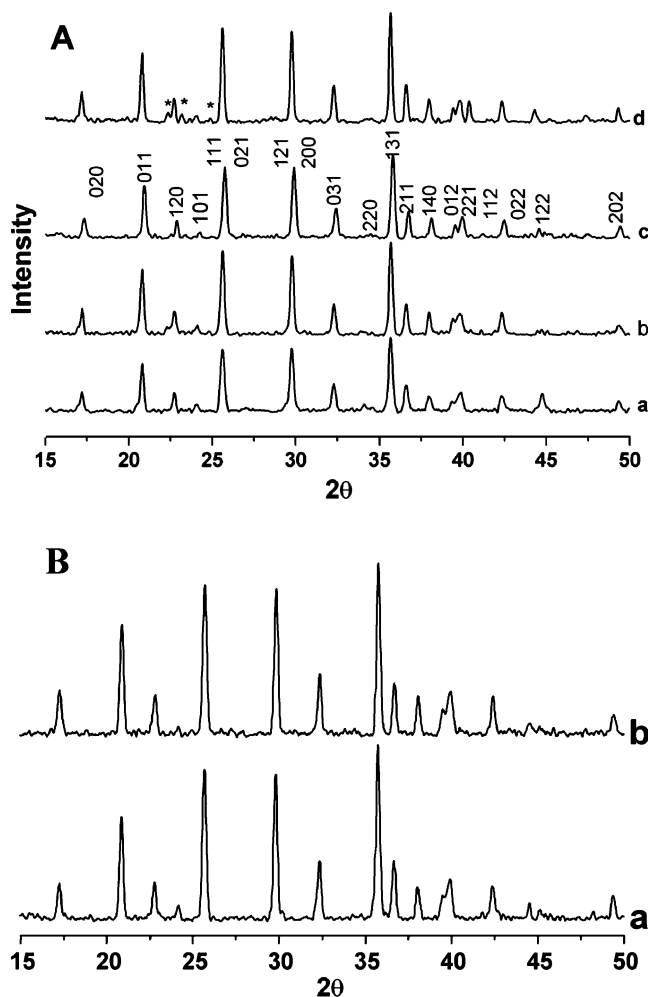


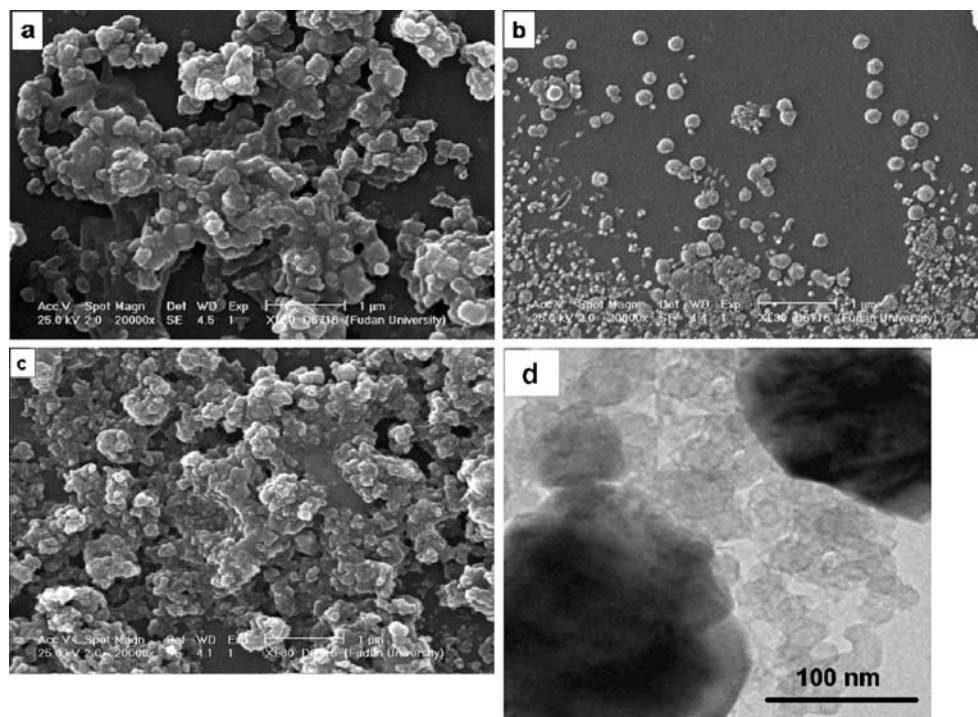
**Fig. 2** XRD patterns of **a**: for  $\text{LiFePO}_4/\text{C}$  samples prepared at different temperatures,  $550$  (a),  $650$  (b),  $750$  (c), and  $850^\circ\text{C}$  (d), and **b**: for the samples of  $\text{LiFePO}_4/\text{C}$  (a),  $\text{Li}_{0.99}\text{Ti}_{0.01}\text{FePO}_4/\text{C}$  (b) composites prepared at  $750^\circ\text{C}$

ite is displayed in Fig. 3d, and it can be found that  $\text{Li}_{0.99}\text{Ti}_{0.01}\text{FePO}_4$  particles are connected with carbon. The molar ratio of Li, Fe, Ti, and P in the sample was measured by ICP method. It can be calculated that the exact molecular formula is  $\text{Li}_{0.984}\text{Ti}_{0.009}\text{Fe}_{0.992}\text{PO}_4$ , which is close to the formula  $\text{Li}_{0.99}\text{Ti}_{0.01}\text{FePO}_4$ . Carbon content in  $\text{Li}_{0.99}\text{Ti}_{0.01}\text{FePO}_4/\text{C}$  was  $4.66\text{ wt.}\%$ , which was determined by the method introduced by Prosini et al. [23]. This implied that a little amount of carbon was lost during heat-treating.

**Table 1** Crystal parameters of samples

Samples	a (Å)	b (Å)	c (Å)
$\text{LiFePO}_4/\text{C}$	5.988	10.294	4.667
$\text{Li}_{0.99}\text{Ti}_{0.01}\text{FePO}_4/\text{C}$	5.982	10.242	4.678

**Fig. 3** SEM images of  $\text{LiFePO}_4/\text{C}$  composite (a),  $\text{Li}_{0.99}\text{Ti}_{0.01}\text{FePO}_4$  (b), and  $\text{Li}_{0.99}\text{Ti}_{0.01}\text{FePO}_4/\text{C}$  composite (c), and TEM image of  $\text{Li}_{0.99}\text{Ti}_{0.01}\text{FePO}_4/\text{C}$  composite (d)



**Electrochemical properties of  $\text{LiFePO}_4/\text{C}$  samples** It has been known that the deintercalation reaction of lithium ion in  $\text{LiFePO}_4$  is  $\text{LiFePO}_4 \leftrightarrow (1-x)\text{LiFePO}_4 + x\text{FePO}_4 + x\text{Li}^+ + xe^-$ , where  $x < 1$ . The theoretical discharge capacity of  $\text{LiFePO}_4$  is 168 mAh/g [1]. Figure 4 shows the influence of heat treatment on the charge and discharge behavior of  $\text{LiFePO}_4/\text{C}$  samples. The sample synthesized at 550 °C performs at low capacity due to incomplete reaction. The discharge capacity increases with increasing temperature. A smooth potential plateau at 3.38 V appears on the discharge curve for the samples prepared at 650 °C, as well as on that

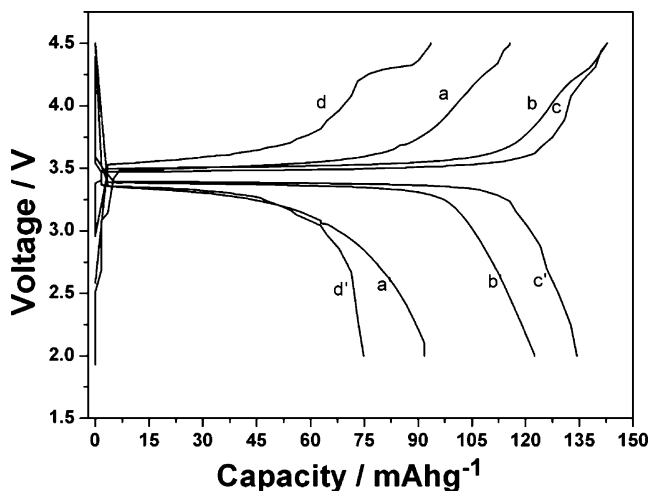


**Fig. 4** Charge and discharge curves of  $\text{LiFePO}_4/\text{C}$  samples calcined at different temperatures: 550 (a, a'), 650 (b, b'), 750 (c, c'), and 850 °C (d, d'), at 0.1 C rate

at 750 °C. Among them, 750 °C is the best synthesized temperature. The sample synthesized at this temperature presents the highest capacity of 132 mAh/g. For the sample treated at 850 °C, a heavy capacity loss was observed, which can be attributed to the structure change and some impurities such as  $\text{Li}_3\text{PO}_4$ , produced at high temperature, as detected in XRD experimental.

The charge/discharge cycle performance of these samples is presented in Fig. 5. It is clear that the cycle behavior of  $\text{LiFePO}_4/\text{C}$  samples is strongly dependent on the calcined temperature. The samples synthesized at 550–750 °C perform stable cycle behavior. The discharge capacity increases with the rise of the heating temperature. But when

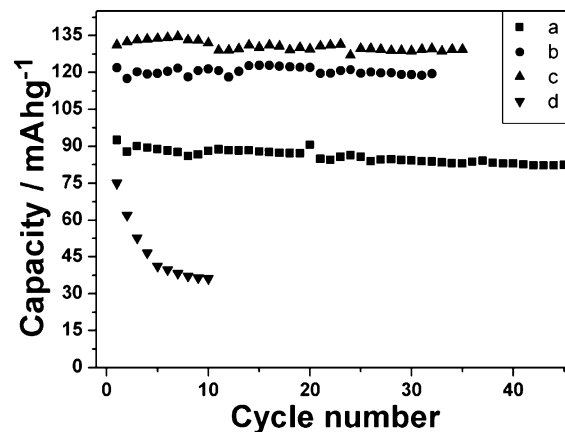


**Fig. 5** Cycle performances for  $\text{LiFePO}_4/\text{C}$  samples synthesized at different temperatures: 550 (a), 650 (b), 750 (c), and 850 °C (d), at 0.1 C rate

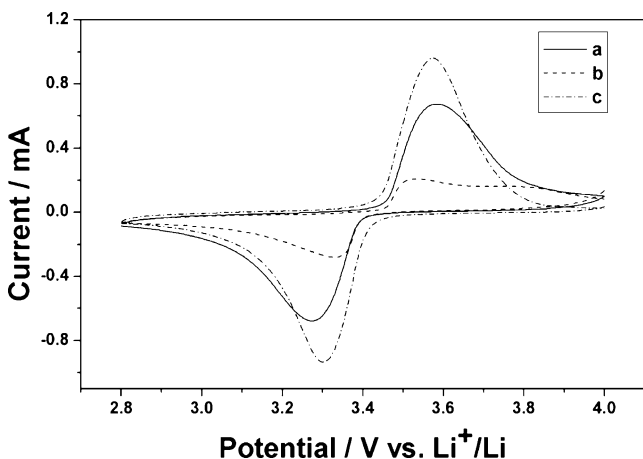


the synthesis temperature reaches 850 °C, the capacity drops quickly. The best preparation temperature is 750 °C, under which the resulting sample presents an initial discharge capacity of 132 mAh/g. After 35 cycles, this discharge capacity remains 129.4 mAh/g.

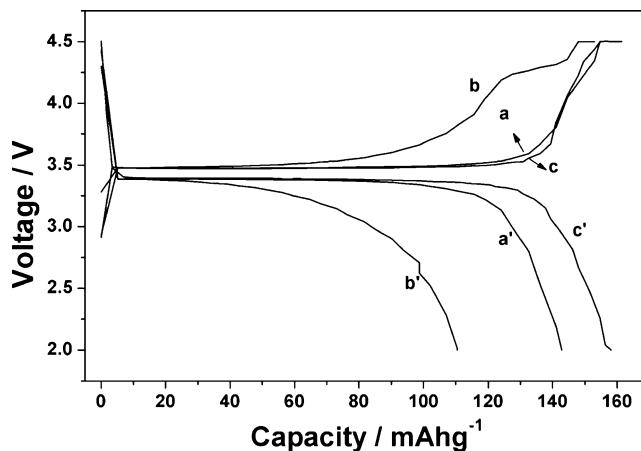
**Electrochemical properties of  $\text{Li}_{0.99}\text{Ti}_{0.01}\text{FePO}_4/\text{C}$  samples** The electrochemical properties of a sample depends greatly upon the sample's composition. Figure 6 presents the cyclic voltammograms of  $\text{LiFePO}_4/\text{C}$ ,  $\text{Li}_{0.99}\text{Ti}_{0.01}\text{FePO}_4$ , and  $\text{Li}_{0.99}\text{Ti}_{0.01}\text{FePO}_4/\text{C}$  composites synthesized at 750 °C. A couple of redox current peaks appear on each voltammogram curve. Among them, the  $\text{Li}_{0.99}\text{Ti}_{0.01}\text{FePO}_4/\text{C}$  sample shows the best electrochemical behavior, with the highest peak current and the narrowest potential margin between the anodic current peak (3.54 V) and the cathodic current peak (3.31 V). The  $\text{Li}_{0.99}\text{Ti}_{0.01}\text{FePO}_4$  sample presents the lowest current peaks, due to the low conductivity without carbon existing.

Figure 7 presents the charge and discharge curves at 0.1 C ( $i=17 \text{ mA/g}$ ) for the samples of  $\text{LiFePO}_4/\text{C}$ ,  $\text{Li}_{0.99}\text{Ti}_{0.01}\text{FePO}_4$ , and  $\text{Li}_{0.99}\text{Ti}_{0.01}\text{FePO}_4/\text{C}$ . One smooth voltage plateau around 3.4 V vs  $\text{Li}^+/\text{Li}$  appears on the charge or discharge curves for all samples.  $\text{Li}_{0.99}\text{Ti}_{0.01}\text{FePO}_4$  presents the lowest discharge capacity, which may be caused by low conductivity between particles without carbon. The best electrochemical behavior was obtained from the sample of  $\text{Li}_{0.99}\text{Ti}_{0.01}\text{FePO}_4/\text{C}$ , not only with the highest discharge capacity of 157 mAh/g but also with the lowest polarization.

The carbon coating and Ti-doping influenced the charge/discharge cycle performance of samples strongly, as shown in Fig. 8a. Both charge and discharge rate are 0.2 C. The  $\text{Li}_{0.99}\text{Ti}_{0.01}\text{FePO}_4/\text{C}$  composite presents the best properties with the original capacity of 154.5 mAh/g. After 120 cycles, it maintains 92% of the initial capacity. This can be attributed to the improvement of the diffusion character by Ti doping and conductivity between particles by carbon



**Fig. 6** Cyclic voltammograms of samples:  $\text{LiFePO}_4/\text{C}$  (a),  $\text{Li}_{0.99}\text{Ti}_{0.01}\text{FePO}_4$  (b), and  $\text{Li}_{0.99}\text{Ti}_{0.01}\text{FePO}_4/\text{C}$  (c) composites. Scan rate 0.1 mV/s



**Fig. 7** Charge and discharge profiles of samples:  $\text{LiFePO}_4/\text{C}$  (a, a'),  $\text{Li}_{0.99}\text{Ti}_{0.01}\text{FePO}_4$  (b, b'), and  $\text{Li}_{0.99}\text{Ti}_{0.01}\text{FePO}_4/\text{C}$  (c, c') composites,  $i=17 \text{ mA/g}$  (0.1 C), voltage range: 2.0–4.5 V

coating. The sample treated only by carbon coating also presents good cycle stability, but the discharge capacity is much lower than that of  $\text{Li}_{0.99}\text{Ti}_{0.01}\text{FePO}_4/\text{C}$ . A sharp capacity decrease was observed for the sample only doped

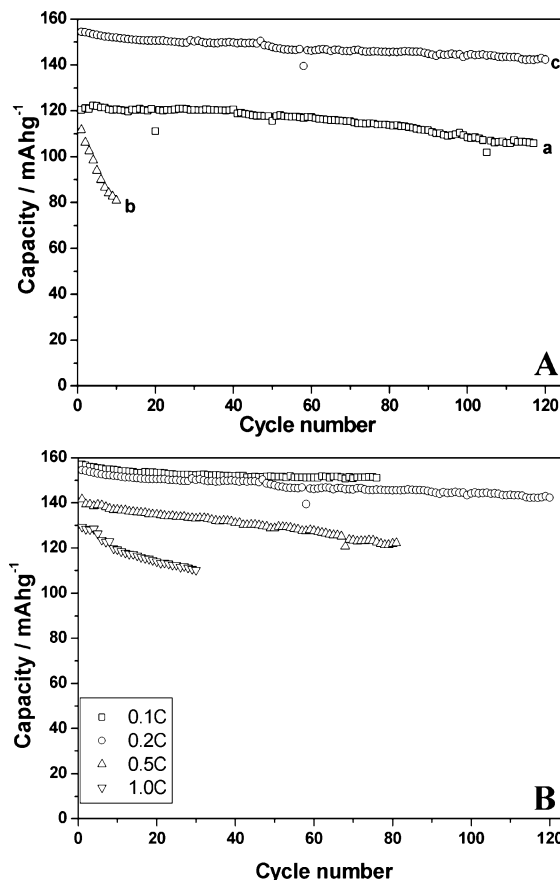


**Fig. 8** Cycle performances for the samples of a:  $\text{LiFePO}_4/\text{C}$  (a),  $\text{Li}_{0.99}\text{Ti}_{0.01}\text{FePO}_4$  (b), and  $\text{Li}_{0.99}\text{Ti}_{0.01}\text{FePO}_4/\text{C}$  (c) composites, at charge/discharge rate of 0.2 C, voltage range 2.0–4.5 V; and b:  $\text{Li}_{0.99}\text{Ti}_{0.01}\text{FePO}_4/\text{C}$  composite at rates of 0.1, 0.2, 0.5, and 1.0 C

with Ti. During the first ten cycles, its capacity reduced by approximately 30%.

The influence of the charge/discharge rate on the cycle performance of  $\text{Li}_{0.99}\text{Ti}_{0.01}\text{FePO}_4/\text{C}$  samples is presented in Fig. 8b. At a lower rate, the samples show excellent cycling stability, such as the first discharge capacity at a rate of 0.1 C, which is 157 mAh/g (about 93.4% of theoretical capacity) and performs very stably. At a 0.2 C rate, it still keeps high discharge capacity and good cycle stability. When the discharge rate rises to 0.5 C, the first discharge capacity is 140 mAh/g, and after 80 cycles, it is reduced to 122 mAh/g. For a discharge rate at 1.0 C, at the first several cycles the discharge capacity remains 130 mAh/g, but in further cycles the capacity decays faster.

The results show that carbon coating together with Ti doping is a very efficient method to improve the electrochemical properties of  $\text{LiFePO}_4$ . The composite material  $\text{Li}_{0.99}\text{Ti}_{0.01}\text{FePO}_4/\text{C}$  can be used as the cathode material for lithium ion batteries.

## Conclusions

Submicron-scale  $\text{Li}_{0.99}\text{Ti}_{0.01}\text{FePO}_4/\text{C}$  composites were synthesized successfully via a solid-state reaction through ball milling and heat treatment. The carbon coating and Ti doping in  $\text{Li}_{0.99}\text{Ti}_{0.01}\text{FePO}_4/\text{C}$  composite promote the discharge capacity and rate capability obviously. The concept of the coeffect of carbon coating and Ti doping is very efficient to improve the electrochemical behavior of  $\text{LiFePO}_4$ . The material  $\text{Li}_{0.99}\text{Ti}_{0.01}\text{FePO}_4/\text{C}$  can be used as the cathode material for lithium ion batteries.

**Acknowledgement** This work was supported by the National Nature Science Foundation of China.

## References

1. Padhi A, Nanjundaswamy KS, Goodenough JB (1997) *J Electrochem Soc* 144:1188
2. Yonemura M, Yamada A, Takei Y, Sonoyama N, Kanno R (2004) *J Electrochem Soc* 151:A1352
3. Wolfenstine J, Allen J (2004) *J Power Sources* 136:150
4. Natalia NB, Kirill GB, Thorsten B, Carsten B, Helmut E, Hartmt F (2004) *J Solid State Electrochem* 8:558
5. Andersson AS, Thomas JO (2001) *J Power Sources* 97–98:498
6. Yamada A, Chung SC, Hinokuma K (2001) *J Electrochem Soc* 148:A224
7. Ravet N, Chouinard Y, Magnan JF, Besner S, Gauthier M, Armand M (2001) *J Power Sources* 97–98:503
8. Huang H, Yin SC, Nazar LF (2001) *Electrochem Solid-State Lett* 4:A170
9. Hsu KF, Tsay SY, Hwang BJ (2005) *J Power Sources* 146:529
10. Yao J, Konstantinov K, Wang GX, Liu HK (2006) *J Solid State Electrochem* 8:558
11. Chung SY, Bloking JT, Chiang YM (2002) *Nat Mater* 1:123
12. Chung SY, Chiang YM (2003) *Electrochem Solid-State Lett* 6: A278
13. Wang GX, Bewlay SL, Konstantinov K, Liu HK, Dou SX, Ahn JH (2004) *Electrochim Acta* 50:443
14. Shi S, Liu L, Ouyang C, Wang D, Wang Z, Chen L, Huang X (2003) *Phys Rev B* 68:195108
15. Ouyang C, Shi S, Wang Z, Huang X, Chen L (2004) *Phys Rev B* 69:104303
16. Herle PS, Ellis B, Coombs N, Nazar LF (2004) *Nat Mater* 3:147
17. Abbate M, Lata SM, Montoro LA, Rosolen JM (2005) *Electrochem Solid-State Lett* 8:A288
18. Wang GX, Bewlay S, Yao J, Ahn JH, Dou SX, Liu HK (2004) *Electrochem Solid-State Lett* 7:A503
19. Wang GX, Bewlay S, Needham SA, Liu HK, Liu RS, Drozd VA, Lee JF, Chen JM (2006) *J Electrochem Soc* 153:A25
20. Wang D, Li H, Shi S, Huang X, Chen L (2005) *Electrochim Acta* 50:2955
21. Liu H, Wu YP, Rahm E, Holze R, Wu HQ (2004) *J Solid State Electrochem* 8:450
22. Chen Z, Dahn JR (2002) *J Electrochem Soc* 149:A1184
23. Prosini PP, Lisi M, Zane D, Pasquali M (2002) *Solid State Ionics* 148:45